High-resolution mass spectrometry provides novel insights into products of human metabolism of organophosphate and brominated flame retardants

Abdallah, Mohamed Abou Elwafa; Zhang, Jinkang; Pawar, Gopal; Viant, Mark R.; Chipman, J. Kevin; D'Silva, Kyle; Bromirski, Maciej; Harrad, Stuart

DOI:
10.1007/s00216-015-8466-z

Document Version
Peer reviewed version

Citation for published version (Harvard):
Abdallah, MAE, Zhang, J, Pawar, G, Viant, MR, Chipman, JK, D'Silva, K, Bromirski, M & Harrad, S 2015, 'High-resolution mass spectrometry provides novel insights into products of human metabolism of organophosphate and brominated flame retardants', *Analytical and Bioanalytical Chemistry*, vol. 407, no. 7, pp. 1871-1883. https://doi.org/10.1007/s00216-015-8466-z

HIGH RESOLUTION MASS SPECTROMETRY PROVIDES NOVEL INSIGHTS INTO PRODUCTS OF HUMAN METABOLISM OF ORGANOPHOSPHATE AND BROMINATED FLAME RETARDANTS

Journal:	*Analytical Chemistry*
Manuscript ID:	ac-2014-041132
Manuscript Type:	Article
Date Submitted by the Author:	04-Nov-2014

Complete List of Authors:	Abdallah, Mohamed; University of Birmingham, Division of Environmental Health & Risk Management Zhang, Jinkang; University of Birmingham, School of Biosciences Pawar, Gopal; University of Birmingham, Division of Environmental Health & Risk Management Viant, Mark; University of Birmingham, School of Biosciences Chipman, James; University of Birmingham, School of Biosciences D'Silva, Kyle; ThermoFisher Scientific, Bromirski, Maciej; ThermoFisher Scientific, Harrad, Stuart; University of Birmingham, Division of Environmental Health & Risk Management

HIGH RESOLUTION MASS SPECTROMETRY PROVIDES NOVEL INSIGHTS INTO PRODUCTS OF HUMAN METABOLISM OF ORGANOPHOSPHATE AND BROMINATED FLAME RETARDANTS

Mohamed Abou-Elwafa Abdallah[1,2*], Jinkang Zhang[3], Gopal Pawar[1], Mark Viant[3], J. Kevin Chipman[3], Kyle D'Silva[4], Maciej Bromirski[4], Stuart Harrad[1]

[1]Division of Environmental Health and Risk Management, School of Geography, Earth and Environmental Sciences, University of Birmingham, Birmingham, B15 2TT, UK.

[2]Department of Analytical Chemistry, Faculty of Pharmacy, Assiut University, 71526 Assiut, Egypt.

[3]School of Biosciences, University of Birmingham, Birmingham, B15 2TT, UK.

[4]Thermo Fisher Scientific (Bremen) GmbH, 28199 Bremen, Germany.

* Corresponding author

Email mae_abdallah@yahoo.co.uk

Tel. +44 121 414 7297

Fax. +44 121 414 3078

Abstract

The high resolution, accurate mass and fast scanning features of the Orbitrap™ mass spectrometer, combined with the separation power of ultrahigh performance liquid chromatography were applied *for the first time* to study the metabolic profiles of several organic flame retardants (FRs) present in indoor dust. To mimic real-life exposure, *in vitro* cultured human hepatocytes were exposed *simultaneously* to various FRs in an indoor dust extract for 24 hours. Target parent FRs, hexabromocyclododecanes (α-, β- and γ-HBCDs), tris-2-chloroethyl phosphate (TCEP), tris (1-chloro-2-propyl) phosphate (TCIPP) and tris (1,3-dichloro-2-propyl) phosphate (TDCIPP), were separated in a single run *for the first time* using alternating positive and negative heated ESI source. Further metabolite separation and identification was achieved using full scan (70,000 FWHM), accurate mass (up to 1 ppm) spectrometry. Structural confirmation was performed via all ion fragmentation (AIF) spectra using the optional higher collisional dissociation (HCD) cell and MS/MS analysis. First insights into human metabolism of HBCDs revealed several hydroxylated and debrominated phase I metabolites, in addition to conjugated phase II glucuronides. Furthermore, various hydroxylated, oxidized and conjugated metabolites of chlorinated phosphorous FRs were identified, leading to the suggestion of α-oxidation as a significant metabolic pathway for these compounds.

1 Introduction

Cellular stress is a general term covering a wide range of molecular changes that cells undergo in response to various stressors. Environmental stressors may include extremes of temperature, mechanical damage and exposure to toxins or xenobiotics (e.g. flame retardant chemicals (FRs)).[1] Several studies have highlighted the importance of indoor dust as a pathway of human exposure to FRs and related persistent organic pollutants (POPs).[2,3] However, few studies have investigated the metabolic pathways of FRs present in indoor dust. Most of these studies have focused on metabolism of polybrominated diphenyl ethers (PBDEs) using animal or human liver microsomes,[4] hepatic S9 fractions[5] and rarely, human hepatocytes.[6] Furthermore, the restrictions on production and usage of PBDEs followed by inclusion of the Penta- and Octa-BDE commercial formulations as persistent organic pollutants (POPs) under Annex A of the UNEP Stockholm Convention on POPs[7] have led to the application of alternative FRs to meet fire safety regulations. Currently, very little is known about the metabolic pathways of alternative FRs in humans. Among these alternatives, the chlorinated alkyl phosphates: tris-2-chloroethyl phosphate (TCEP), tris (1-chloro-2-propyl) phosphate (TCIPP) and tris (1,3-dichloro-2-propyl) phosphate (TDCIPP), in addition to hexabromocyclododecane (HBCD); are associated with a variety of applications in a wide range of consumer products.

TCEP, TCIPP and TDCIPP have been widely applied as FRs in polyurethane foam for domestic, public, and automotive applications with an estimated annual consumption of 91,000 tonnes in 2006.[8] Each were subject to an EU risk assessment process under an Existing Substances Regulation (EEC 793/93). As a result, all 3 compounds were classified as persistent organic compounds in the aquatic environment and reported to fulfil PBT criteria.[9] In addition, several studies have reported them to display adverse

effects including reproductive toxicity and carcinogenic effects on lab animals.[8] Hence, TCEP is classified by the EU as a "potential human carcinogen",[10] while TDCIPP is classified under regulation EC 1272/2008 as a category 2 carcinogen with hazard statement H351 "suspected of causing cancer".[11] Information on the biotransformation pathways of organophosphate flame retardants (PFRs) is limited. While phosphoric acid diesters were the major metabolites of TDCIPP and TCEP identified in rat urine,[12] a recent *in vitro* study using human liver microsomes and S9 fractions reported the replacement of Cl with OH followed by conjugation as a major metabolic pathway for TCEP and TCIPP.[13]

HBCD is an additive FR widely applied in expanded and extruded polystyrene foams (EPS/XPS) used for thermal insulation of buildings and to a lesser extent in the backcoating of fabrics and high impact polystyrene casing for electrical goods. The commercial formulations consist mainly of α-, β-, and γ-diastereomers with γ-predominant (>70% ΣHBCD). HBCD has low water solubility (49, 15, and 2 μg L^{-1} for α-, β-, and γ-HBCD respectively), a fairly low vapor pressure (6.27×10^{-5} Pa) and is persistent. It can therefore bioaccumulate and undergo long-range transport.[14] Oral exposure to HBCDs was reported to induce hepatic cytochrome P450 enzymes and alter the normal uptake of neurotransmitters in rat brain. It can cause disruption of thyroid function, the reproductive system, nerve function and development in various classes of vertebrates.[15] Therefore, HBCD was recently included in Annex A of the Stockholm Convention on POPs with an exemption for use in EPS/XPS in buildings.[7] Currently, little is known about the metabolism of HBCDs in humans or other biota. Recent *in vitro* studies in rat and trout liver S9 fractions showed oxidation (hydroxylation) and reductive debromination as the main biotransformation pathways,[16] which was in agreement with *in vivo* studies in Wistar rats[17] and female mice.[18] To the authors'

knowledge, there exists hitherto, no studies of HBCD metabolism in human liver preparations. Moreover, there are no studies on the biotransformation of HBCDs, TCEP, TCIPP, and TDCIPP in indoor dust by human hepatocytes which contain the full system for Phase I and Phase II metabolic reactions. Furthermore, very little is known about the metabolic behavior of human liver cells upon concomitant exposure to multiple stressors which mimic the real life situation. Biotransformation of FRs can be a major determinant of the toxicological and bioaccumulative properties of these xenobiotics in humans.

Although targeted routine analysis of HBCD diastereomers and chlorinated alkyl phosphates using various LC-MS and GC-MS techniques is well-documented,[8,15] separation and identification of metabolites following exposure of human hepatocytes to a complex mixture of the target FRs requires use of high resolution mass spectrometric methods (HR-MS). While the application of time-of-flight (TOF-MS) coupled to HPLC to study the *in vitro* biotransformation of individual chlorinated alkyl phosphates has been recently reported;[13] the ability of ultra high mass resolution mass spectrometric methods like Orbitrap-MS to inform understanding of human metabolism of FRs has not yet been evaluated. The mass resolution of Orbitrap-MS (up to 140,000 full width at half maximum (FWHM)) and mass accuracy (up to 1 ppm), provides accurate mass measurements facilitating resolution of target analytes from background matrix interferences and isobaric compounds. Such capacity to obtain mass spectra with high mass accuracy at sufficient mass resolution and scan rates, opens substantial opportunities for combining targeted analysis with unbiased metabolite profiling which can provide new perspectives in metabolite analysis.[19] Review of the available literature on *in vitro* metabolism of FRs present in indoor dust shows that studies were carried out via exposure of the metabolising system (i.e. liver microsomes, liver S9 fractions,

hepatocytes and/or liver slices) to a single contaminant or a small group of closely related contaminants (e.g. HBCDs).[16,20] This simplified approach may allow for the detection and identification of the small number of metabolites formed using the most commonly available low/medium resolution MS or MS/MS systems. However, this might not closely reflect the *in vivo* situation where the metabolising system is simultaneously exposed to a wide range of various xenobiotics, which may greatly influence both the activity (e.g. induction or suppression) of the enzymes and the nature of the produced metabolites (i.e. presence of preferential substrates for certain enzyme groups). Nevertheless, separation and identification of the complex metabolites mixture resulting from simultaneous exposure of hepatocytes to a wide range of contaminants present in indoor dust, needs a combination of high performance chromatographic separation and ultra high resolution mass spectrometry.

Against this backdrop, the aim of the current work was to study *for the first time* the metabolic profiles of HBCDs, TCEP, TCIPP and TDCIPP in indoor dust applied *concomitantly* to human hepatocyte cultures using UPLC-Orbitrap™-MS.

2 Experimental

2.1 Chemicals and reagents

All chemicals were HPLC grade obtained from Sigma-Aldrich Chemical Company (UK) unless otherwise stated.

2.2 Cell culture

Human HepG2/C3A cells were generously provided by Prof. Ronny Blust from the University of Antwerp, Belgium. HepG2/C3A cells were cultured in William's E medium(Sigma, UK) supplemented with 5% heat-inactivated fetal bovine serum (FBS)

(APP, Germany), 100 U penicillin/mL and 100 µg streptomycin/mL (APP, Germany), 4µM L-glutamine (APP, Germany) and 0.4 µM sodium pyruvate (Sigma, UK) and incubated in 37°C with humidified air containing 5% CO_2. Cells were digested with 0.25% trypsin-EDTA and sub-cultured at 80% to 90% confluence exponentially growing HepG2/C3A cells were used for all assays.

The potential cytotoxicity of HBCD to HepG2/C3A cells was evaluated by the CCK-8 assay using a commercial kit, according to the manufacturers' instruction (Dojindo Laboratories, Kumamoto, Japan).

2.3 Dosing solutions

The dosing solutions for this study were prepared to mimic real-life exposure of a 12.3 kg toddler to indoor dust assuming a high dust ingestion scenario (200 mg dust day^{-1}).[21] We used standard NIST SRM 2585 dust with known indicative values for all target compounds (Table SI-1). 240 mg of NIST SRM 2585 dust were extracted using pressurized liquid extraction (Dionex ASE 350, Sunnyvale, CA, USA) according to a previously reported method.[22] The extract was concentrated under a gentle stream of nitrogent, followed by solvent exchange to 2 mL of DMSO using 500 µL of toluene as a "keeper" to minimize analyte loss (D1). Another dosing solution (D2) containing 100 times the concentrations of target analytes in D1 was prepared by appropriate dilution of α-HBCD, β-HBCD, γ-HBCD, TCEP, TCIPP, and TDCIPP reference standards (Wellington Laboratories Inc., ON, Canada) with DMSO. D2 was used to mimic episodic high dose exposure which can be several orders of magnitude higher than average exposure scenarios. [23]

2.4 Human hepatocytes exposure experiments

HepG2/C3A cells were seeded into 6 well plates at density of 10^6 cells in 2 mL culture media per well. After 24 hours acclimatization, cells were exposed to D1 or D2 (10 µL in

DMSO added into 2 mL media) and incubated at 37°C with humidified air containing 5% CO_2. DMSO (10 µL) as vehicle was added into the same volume media as a control, while 10 µL of D1 or D2 were also incubated alone with the culture media on the well plates adjacent to the hepatocytes and analyzed at the end of exposure to determine "real" exposure concentrations for QA/QC purposes (the final concentration of DMSO was 0.5% (v/v) in all treatments). All experiments were performed in triplicate. After 24 hours exposure, cells were harvested and kept frozen at -80°C until analysis.

2.5 Sample extraction

Samples were spiked with 2 mL of methanol and extracted by vortexing for 60 seconds, followed by ultrasonication for 5 minutes and centrifugation at 4,000 *g* for 3 minutes. This extraction cycle was repeated twice before the combined methanol extracts were reduced under a gentle stream of N_2 to 150 µL in a HPLC vial.

2.6 Instrumental Analysis

Chromatographic analysis was achieved using a dual pump Ultimate 3000™ (ThermoScientific, Bremen, Germany) UHPLC system equipped with an Ultimate 3000™ XRS autosampler. Analyte separation was achieved on an Accucore™ RP-MS column (100 x 2.1 cm, 2.6 µm, ThermoScientific, Bremen, Germany) using a mobile phase of 1 mM ammonium acetate (mobile phase A) and Methanol (mobile phase B), each modified with 0.1% formic acid. The elution programme commenced with 25% B ramped up to 50% B over 0.5 min, then increased linearly to 100% B over 6 minutes. This was held for 4 minutes, then decreased to 50% B over 0.5 min and kept at this composition (to equilibriate the column) for a further 1 minute. Overall analysis time was 12 minutes using a constant flow rate of 0.18 mL min^{-1}. The injection volume was 10 µL and the column maintained at 37 °C throughout.

Identification of target analytes (HBCDs, TCEP, TCIPP and TDCIPP) and their metabolites was performed using an Exactive™ Plus Orbitrap™ mass spectrometer (Thermo Scientific, Bremen, Germany) using an ESI source operated in both positive and negative ionization modes.

Due to the lack of reference standards, high resolution full scan mass spectra were used to identify metabolites. Based on the chemical structures of individual studied substrates and the enzyme families (phase I and II metabolism) present in human hepatocytes, a database containing the molecular structures of all theoretically possible metabolites was prepared and saved in TraceFinder™ software. Three successive filters were set in the software for initial metabolite identification:

i. The peak signal to noise ratio (S/N) must exceed 10:1.
ii. The *m/z* value of the molecular ion peak must be within 10 ppm of its theoretical value.
iii. The Br or Cl isotope pattern must match within 5 % of the theoretically predicted abundances.

The identity of potential metabolites were confirmed via all ion fragmentation (AIF) using the higher collisional dissociation (HCD) cell. Thermo Xcalibur™ and TraceFinder™ 3.0 software was used for raw data interpretation and for targeting/identification of metabolites. The fragmentation patterns obtained from each metabolite provided additional information for structural elucidation. Further confirmation of metabolite structures were achieved via MS/MS analysis using the parent (nominal) mass from the Orbitrap full scan and the most predominant fragment obtained from the AIF analysis. Confirmatory tandem mass analyses were performed using a AB Sciex API 2000™ triple quadrupole mass spectrometer equipped with a TurboIonSpray® source used in the multiple reaction monitoring (MRM) mode. Source

and compound specific parameters were adjusted for each parent compound (i.e. HBCDs, TCEP, TCIPP and TDCIPP) via direct infusion experiments (2 ng μL^{-1} standard solution each, in methanol) using a built-in Harvard syringe pump at a flow rate of 10 µL min^{-1} (Table SI-2).

3 Results and discussion

3.1 Optimization of instrumental parameters

Due to the lack of reference standards for metabolites of the target compounds, instrumental parameters were initially optimized using standard solutions of the parent analytes. While several studies exist for the analysis of HBCDs,[15] with fewer reporting the analysis of chlorinated alkyl phosphates using LC/MS based techniques.[8]; this is the first study to attempt separation and identification of all target compounds within the same run. Several mobile phase gradients with different proportions of water, acetonitrile and methanol were tested, with various percentages of different additives including formic acid, ammonium acetate and ammonium chloride. While inclusion of acetonitrile in the mobile phase enhanced the resolution between β- and γ-HBCDs, it was not essential for baseline separation and caused a general decrease in the ESI signal intensity for all target analytes. Therefore, acetonitrile was removed from the mobile phase and baseline separation of all target compounds within a reasonable run time (12 min) was achieved using the mobile phase program described under section 2.6 (Figure 1).

Several C_{18}-RP columns (100 x 2.1 cm) with different particle sizes, namely: Syncronis™ (1.7 µm), Hypersil gold™ (1.9 µm), Acclaim™ (2.2 µm), Hypersil™ (2.4 µm) and Accucore™ (2.6 µm) were tested for separation of the studied compounds. While all the tested columns provided baseline separation, better resolution factors with reasonable retention of the target analytes within acceptable pressure range, was achieved using

the Accucore™ column (Figure 1). Columns with smaller stationary phase particle size required very high pressures - accompanied by higher column temperatures - throughout the run, with potential for solvent leaks or emergency termination of the run should the pressure limit be exceeded.

Following chromatographic separation, the analytes were introduced to the Orbitrap-MS via a heated electrospray ionization (HESI) source with fast polarity switching between positive (PFRs) and negative (HBCDs) ionization modes. Optimised ESI source parameters are provided in table 1. The ions were then guided via a complex optical system to the C-trap which allows storage of a significant ion population prior to quick injection into the Orbitrap analyzer in short pulses, so that each mass-to-charge (m/z) population forms a sub-microsecond pulse. In this study, the automated gain control (AGC) was set to 3×10^6 ions for full scan analysis and 1×10^6 ions for semi-quantitative analysis. The Orbitrap-MS can provide high mass accuracy (typically less than 3 ppm) with high resolution. While the maximum mass resolution of the Orbitrap-MS is 140,000 FWHM, this resulted in highly deformed peaks and a long scan time. Therefore, a mass resolution of 70,000 FWHM was selected for full scan analysis while a mass of 35,000 FWHM was used for semi-quantitative analysis. Due to the lack of reference standards for putative Phase-I and Phase-II metabolites of the target compounds, identification of metabolites was based on their accurate mass provided by: a full MS scan, their fragmentation pattern obtained using the optional high energy collisional dissociation (HCD) cell, isotope patterns which reflect the presence of naturally occurring heavier isotopes of common atom (e.g. ^{81}Br or ^{37}Cl) (Figure SI-1), and confirmational MS/MS analysis (Table SI-2).

3.2 HBCD metabolic profile

Following incubation of α-, β- and γ- HBCDs (present in a SRM2585 dust extract) with human hepatocytes, 2 peaks for pentabromocyclododecene (PBCD) and 1 peak for tetrabromocyclododecadiene (TBCD) were observed. The metabolites were identified and linked to their parent compounds based on: the acquired accurate mass spectra (Figure 2), AIF fragmentation pattern, retention time windows (on the basis that peaks of the lower brominated compounds will appear before the less polar parent compound) and LC-ESI-MS/MS analysis using the respective MRM for each metabolite (table SI-2). While this study is the first to report on HBCD metabolism in human models; PBCDs and TBCDs metabolites were previously reported in rat[17] and mice[18] *in vivo* studies. Moreover, we have recently reported on the formation of 3 PBCDs and 2 TBCDs following incubation of α-, β- and γ- HBCDs with rat S9 fractions.[16] The debrominated metabolites have also been identified in human milk samples from UK[24] and USA[25].

As a result of phase I metabolism, several hydroxylation products of HBCDs, PBCDs and TBCDs were identified with a major ion cluster at $[M+16]^-$ and a predominant fragment at m/z = 80.9153 corresponding to the Br^- ion (Figure 2). One di-hydroxylated and five mono-hydroxylated metabolites were identified for parent HBCDs; two mono-hydroxyl metabolites were identified for PBCDs and one mono-hydroxyl metabolite for TBCD (Table 2). Previous *in vitro* studies have reported several hydroxylated metabolites of HBCDs and its debrominated metabolites using induced rat liver microsomes[26] and S9 fractions.[16] Brandsma *et al*. identified mono-hydroxyl metabolites of both PBCD and TBCD in male Wistar rats[17]. Another *in vivo* metabolic study in female mice detected both mono- and di- hydroxyl metabolites of PBCD but no hydroxyl TBCD derivatives[18]. Theoretically, the 6 main HBCD enantiomers can produce 48 possible allylic PBCD

structures and each HBCD enantiomer can lead to a maximum of six different diastereomeric mono- hydroxyl HBCD structures which can result in a huge number of possible di-hydroxyl HBCDs.[26] Therefore, while the different number of metabolites identified in various studies may be attributed to species-specific variability in phase I metabolism and different exposure conditions,[16], co-elution of one or more HBCD metabolites cannot be excluded in the absence of reference standards for these compounds. Collectively, these results support our previous findings that while cytochrome P450 enzymes are involved in the stereoselective phase I oxidative metabolism of HBCDs; the detection of penta- and tetra- brominated metabolites together with their hydroxylated products indicate sequential reductive debromination (not catalysed by cytochrome P450 enzymes[27]) as a potential pathway of HBCD metabolism. Despite mounting evidence of the involvement of deiodinase enzymes in the metabolic debromination of PBDEs[28,29], further research is required prior to comparing these studies to HBCDs, due to the aliphatic nature of HBCDs as opposed to the aromatic structure of PBDEs.

As a result of phase II metabolism, glucuronide conjugates were identified for the first time for both HBCDs and PBCDs at $[M+176]^-$. Glucuronide formation was identified via accurate MS spectra and matching isotope fractions (Figure 3). Conformatory AIF MS2 spectra showed characteristic glucuronide fragments at m/z = 176 and 113[30] (Figure SI-2), which were used for confirmatory MS/MS analysis of the formed conjugates. An *in vivo* study identified a methylmercapturate conjugate of TBCD in the urine of female mice exposed orally to γ-HBCD.[18] However, no mercapturate or sulfate conjugates could be identified in this study which may indicate species-specific differences in HBCD metabolism. To the author's knowledge, this is the first study of HBCD metabolism in humans, which precludes comparison of results within the same species.

3.3 TCEP metabolic profile

Several TCEP metabolites were identified using accurate MS spectra and confirmatory Cl isotope fractions (Figure 4). Based on relative peak area to the parent compound, bis(2-chloroethyl) hydrogen phosphate (BCEP) (Table SI-3) appeared the major metabolite formed by the studied human cell lines. This is in agreement with previous *in vivo* metabolic studies in rats and mice,[31] and a previous *in vitro* study using human and rat liver preparations.[32] In addition, a hydroxylated metabolite, bis(2-chloroethyl) 2-hydroxyethyl phosphate (TCEP-M1), and its oxidation product, bis(2-chloroethyl) carboxymethyl phosphate (TCEP-M2), were positively identified (Figure 4 and Table SI-3). TCEP-M1 was previously identified as a major TCEP metabolite following incubation with human liver microsomes,[13] While TCEP-M2 was found in rat urine exposed to TCEP via gavage.[31] Therefore, we hypothesize α-oxidation as a significant metabolic pathway of TCEP in human hepatocytes (Figure 5). The reaction starts with α-hydroxylation of a terminal chloromethyl group resulting in an unstable chlorohydrin intermediate (IM-1), which loses a HCl moiety to produce an aldehyde (IM-2). The formed aldehyde can then be oxidized by an aldehyde dehydrogenase to produce TCEP-M2, or reduced by an alcohol dehydrogenase to the corresponding alcohol (TCEP-M1) (Figure 5 and Table SI-3). Metabolic α-oxidation has been previously reported for halomethyl groups in other chemicals e.g. 1-chloropropane[33] and was also suggested for TCEP in rats.[31]

Phase II metabolism resulted in the formation of a glutathione conjugate of the parent compound TCEP (Figure 4). Identification of the glutathione conjugate was confirmed via LC-MS/MS analysis in neutral loss mode where the characteristic fractions of m/z = 308 and 179 (neutral loss of 129) were observed in positive ion ESI mode (Figure SI-3). Moreover, the glucoronide conjugate of TCEP-M1 was also identified (Figure 4 and

Table SI-3). This conjugate was previously reported in rat and mice urine[31] and suggested following *in vitro* exposure of rat and human liver preparations to TCEP.[32]

3.4 TCIPP metabolic profile

Very little is known about the biotransformation of TCIPP. To the authors' knowledge, there is only one recent paper studying the biotransformation of TCIPP by human liver microsomes and S9 fractions.[13] In the current work, bis(1-chloro-2-propyl) hydrogen phosphate (BCIPP) was identified as a major metabolite by human HepG2 cells (Table 3). Interestingly, two isomeric peaks were observed for BCIPP in samples exposed to the dust extract, while only one BCIPP peak was found in samples exposed to the standard mixture D2. Van den Eede et al. reported two BCIPP isomers after incubating human liver microsomes with a TCIPP mixture of tris(1-chloro-2-propyl) phosphate (>66%) and tris(1-chloropropyl) phosphate (~30%). The formation of two BCIPP isomers was attributed to exposure of the microsomes to two TCIPP isomers.[13] Therefore, the detection of one BCIPP isomer following exposure of human HepG2 cells to D2, can be attributed to the presence of pure tris(1-chloro-2-propyl) phosphate in the Wellington® standard for TCIPP, which was used to prepare the dosing mixture D2 in this study.

Furthermore, a hydroxylated metabolite, bis(1-chloro-2-propyl) hydroxy 2-propyl phosphate (TCEP-M1), and a carboxylic acid, bis(1-chloro-2-propyl) carboxy 2-ethyl phosphate (TCEP-M2), were also identified (Table 3). This suggests that α-oxidation (Figure 5) may constitute a major metabolic pathway for TCIPP in human hepatocytes.

As a result of Phase II metabolism, the glutathione conjugate of TCIPP was identified (Table 3). However, no glucuronide or sulfate conjugates could be confirmed.

3.5 TDCIPP metabolic profile

Biotransformation of TDCIPP in indoor dust by human hepatocytes followed a similar profile to that observed for TCEP and TCIPP (Table 4). The diester, bis(1,3-dichloro-2-propyl) hydrogen phosphate (BDCIPP), was the major metabolite formed after 24 hours of exposure (based on the relative peak area to that of the parent TDCIPP). This is in agreement with a previous *in vivo* study, which reported BDCIPP as the major urinary, fecal and biliary metabolite in rats following intravenous administration of radiolabeled TDCIPP.[34] Another *in vitro* study also reported BDCIPP as the major metabolite of TDCIPP by human liver microsomes.[13] In addition to the hydroxylated metabolite (TDCIPP-M1) and the carboxylic acid metabolite (TDCIPP-M2), the monoester, 1,3-dichloro-2-propyl dihydrogen phosphate (DCIPP), was also identified (Table 4). Further hydrolysis of BDCIPP by esterases was previously suggested following *in vitro* incubation of TDCIPP with human liver microsomes.[35]

The glutathione conjugate of TDCIPP was identified as a result of phase II metabolism (Table 4). This is in agreement with the results of previous *in vitro* studies using human liver microsomes.[13,35]

4 Conclusion

A novel multi-residue analytical method was developed and applied to study the metabolic products formed when human HepG2 cell lines were challenged simultaneously – for the first time - with several widely-used organic flame retardants present in indoor dust. To mimic real-life exposure scenarios, human hepatocytes were concomitantly exposed for 24 hours to α-HBCD, β-HBCD, γ-HBCD, TCEP, TCIPP, and TDCIPP extracted from indoor dust. To identify the large number of metabolites formed, an Exactive™ Plus Orbitrap™ high resolution mass spectrometer was applied following

chromatographic separation via UPLC. For the first time, target parent compounds were separated and monitored in a single run using an alternating positive and negative heated ESI source. Further metabolite separation and identification was performed using the high resolution (70,000 FWHM) accurate mass (up to 1 ppm) features of the Orbitrap™-MS. Structural confirmation of the detected metabolites was achieved via all ion fragmentation (AIF) spectra using the optional higher collisional dissociation (HCD) cell of the MS. Hepatic metabolism of HBCDs in human was investigated for the first time. Several hydroxylated and debrominated phase I metabolites were identified, while conjugated phase II glucuronides of HBCDs were also confirmed. Hydroxylated, oxidized and conjugated metabolites of chlorinated phosphorous flame retardants were also observed and α-oxidation was proposed as a metabolic pathway for target PFRs in human hepatocytes.

5 Supporting Information

Further details on analytical method optimization, QA/QC measurements and structural confirmation of metabolites are provided as supporting information.

6 Acknowledgement

The research leading to these results has received funding from the European Union Seventh Framework Programme FP7/2007-2013 under grant agreements PIIF-GA-2012-327232 (ADAPT project), 316665 (A-TEAM project), and 264600 (INFLAME project).

References

(1) Lokke, H.; Ragas, A. M. J.; Holmstrup, M. *Toxicology* **2013**, *313*, 73-82.
(2) Trudel, D.; Scheringer, M.; von Goetz, N.; Hungerbuehler, K. *Environ Sci Technol* **2011**, *45*, 2391-2397.
(3) Cao, Z. G.; Xu, F. C.; Covaci, A.; Wu, M.; Wang, H. Z.; Yu, G.; Wang, B.; Deng, S. B.; Huang, J.; Wang, X. Y. *Environ Sci Technol* **2014**, *48*, 8839-8846.
(4) Hakk, H.; Letcher, R. J. *Environ Int* **2003**, *29*, 801-828.
(5) Browne, E. P.; Stapleton, H. M.; Kelly, S. M.; Tilton, S. C.; Gallagher, E. P. *Aquat Toxicol* **2009**, *92*, 281-287.
(6) Stapleton, H. M.; Kelly, S. M.; Pei, R.; Letcher, R. J.; Gunsch, C. *Environ Health Persp* **2009**, *117*, 197-202.
(7) United Nations Environment Programme (UNEP). *http://chm.pops.int/TheConvention/POPsReviewCommittee/OverviewandMandate/tabid/2806/Default.aspx* **2014**.
(8) van der Veen, I.; de Boer, J. *Chemosphere* **2012**, *88*, 1119-1153.
(9) Regnery, J.; Puettmann, W.; Merz, C.; Berthold, G. *J Environ Monitor* **2011**, *13*, 347-354.
(10) Regnery, J.; Puttmann, W. *Water Res* **2010**, *44*, 4097-4104.
(11) ECHA. *http://echa.europa.eu/documents/10162/0410f4e3-7838-4819-b321-f9d75d3a9cce (accessed 19-6-2012)* **2010**.
(12) Environmental Health Criteria. *International Programme on Chemical Safety. World Health Organization, Geneva,* **1995**, *172*.
(13) Van den Eede, N.; Maho, W.; Erratico, C.; Neels, H.; Covaci, A. *Toxicol Lett* **2013**, *223*, 9-15.
(14) KEMI. *R044_0710_env_hh.doc; Sundbyberg, Sweden* **2007**.
(15) Marvin, C. H.; Tomy, G. T.; Armitage, J. M.; Arnot, J. A.; McCarty, L.; Covaci, A.; Palace, V. *Environ Sci Technol* **2011**, *45*, 8613-8623.
(16) Abdallah, M. A.-E.; Uchea, C.; Chipman, J. K.; Harrad, S. *Environ Sci Technol* **2014**, *48*, 2732-2740.
(17) Brandsma, S. H.; van der Ven, L. T. M.; de Boer, J.; Leonards, P. E. G. *Environ Sci Technol* **2009**, *43*, 6058-6063.
(18) Hakk, H.; Szabo, D. T.; Huwe, J.; Diliberto, J.; Birnbaum, L. S. *Environ Sci Technol* **2012**, *46*, 13494-13503.
(19) Werner, E.; Croixmarie, V.; Umbdenstock, T.; Ezan, E.; Chaminade, P.; Tabet, J. C.; Junot, C. *Analytical Chemistry* **2008**, *80*, 4918-4932.
(20) Alves, A.; Kucharska, A.; Erratico, C.; Xu, F. C.; Den Hond, E.; Koppen, G.; Vanermen, G.; Covaci, A.; Voorspoels, S. *Anal Bioanal Chem* **2014**, *406*, 4063-4088.
(21) Jones-Otazo, H. A.; Clarke, J. P.; Diamond, M. L.; Archbold, J. A.; Ferguson, G.; Harner, T.; Richardson, G. M.; Ryan, J. J.; Wilford, B. *Environ Sci Technol* **2005**, *39*, 5121-5130.
(22) Harrad, S.; Abdallah, M. A.-E. *Chemosphere* **2011**, *82*, 1240-1245.
(23) Abdallah, M. A.; Harrad, S. *Environ Int* **2009**, *35*, 870-876.
(24) Abdallah, M. A.; Harrad, S. *Environ Int* **2011**, *37*, 443-448.
(25) Carignan, C. C.; Abdallah, M. A.; Wu, N.; Heiger-Bernays, W.; McClean, M. D.; Harrad, S.; Webster, T. F. *Environ Sci Technol* **2012**, *46*, 12146-12153.
(26) Esslinger, S.; Becker, R.; Maul, R.; Nehls, I. *Environ Sci Technol* **2011**, *45*, 3938-3944.
(27) Benedict, R. T.; Stapleton, H. M.; Letcher, R. J.; Mitchelmore, C. L. *Chemosphere* **2007**, *69*, 987-993.
(28) Butt, C. M.; Wang, D.; Stapleton, H. M. *Toxicol Sci* **2011**.

(29) Szabo, D. T.; Richardson, V. M.; Ross, D. G.; Diliberto, J. J.; Kodavanti, P. R. S.; Birnbaum, L. S. *Toxicol Sci* **2009**, *107*, 27-39.
(30) Holcapek, M.; Kolarova, L.; Nobilis, M. *Anal Bioanal Chem* **2008**, *391*, 59-78.
(31) Burka, L. T.; Sanders, J. M.; Herr, D. W.; Matthews, H. B. *Drug Metabolism and Disposition* **1991**, *19*, 443-447.
(32) Chapman, D. E.; Michener, S. R.; Powis, G. *Fundamental and Applied Toxicology* **1991**, *17*, 215-224.
(33) Stubbings, W. A.; Harrad, S. *Environ Int* **2014**, *71*, 164-175.
(34) Lynn, R. K.; Wong, K.; Garviegould, C.; Kennish, J. M. *Drug Metabolism and Disposition* **1981**, *9*, 434-441.
(35) Cooper, E.; Stapleton, H. *SETAC North America 32nd Annual Meeting. http://orbit.dtu.dk/fedora/objects/orbit:105810/datastreams/file_6352082/content* **2011**, 176.

7 Tables

Table 1: Optimized HESI-Orbitrap-MS parameters for analysis of target FRs.

Parameter	Value
Capillary temperature (°C)	300
Source heater temperature (°C)	300
Electrospray voltage (V)	4500
Sheath gas flow (a.u.)*	15
Auxiliary gas flow (a.u.)*	10
S-lens frequency (Hz)	50
Maximum injection time (ms)	80
Automatic gain control (ions)	3×10^6
HCG energy (ev)	35
MS resolution (FWHM)	70000

Table 2: Metabolic profile of HBCDs by human HepG2 cell lines.

Name	Retention time (mins)	Molecular formula	Chemical structure	Molecular ion $[M-H]^-$	Theoretical mass
HBCD (3 isomers)	8.50, 8.69, 8.84	$C_{12}H_{18}Br_6$	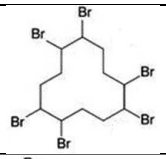	640.6378	640.6369
PBCD (2 isomers)	7.19, 7.58	$C_{12}H_{17}Br_5$	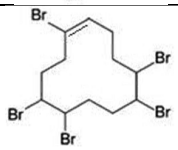	560.6883	560.7186
TBCD	6.63	$C_{12}H_{16}Br_4$	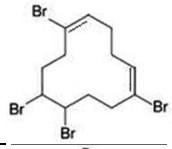	478.7618	478.7866
HBCD-OH (5 isomers)	5.89, 6.09, 6.38, 6.72, 7.11	$C_{12}H_{18}Br_6O$	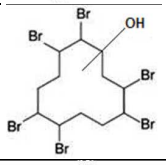	656.6370	656.6318
Di-hydroxyl HBCD	5.08	$C_{12}H_{18}Br_6O_2$	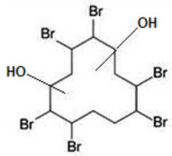	672.6412	672.6346
PBCD-OH (2 isomers)	5.48, 5.71	$C_{12}H_{17}Br_5O$	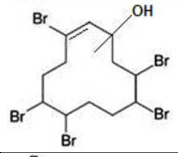	574.7077	574.7805
TBCD-OH	5.29	$C_{12}H_{16}Br_4O$	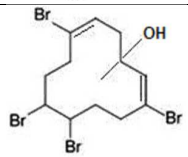	494.8342	494.7816
HBCD-O-Glu (2 isomers)	4.49, 4.68	$C_{18}H_{26}Br_6O_7$	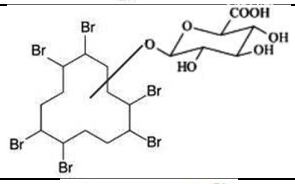	832.6766	832.6640
PBCD-O-Glu	3.22	$C_{18}H_{25}Br_5O_7$	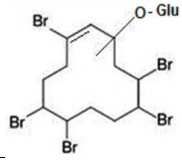	750.7149	750.7398

Table 3: Metabolic profile of TCIPP by human HepG2 cell lines.

Name	Retention time (mins)	Molecular formula	Chemical structure	Molecular ion $[M+H]^+$	Theoretical mass
TCIPP	5.58	$C_9H_{18}Cl_3O_4P$	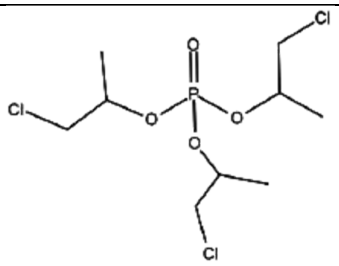	327.0081	327.0009
BCIPP	1.86	$C_6H_{13}Cl_2O_4P$	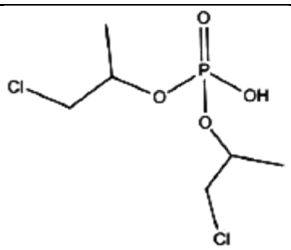	250.9929	251.0002
TCIPP-M1	3.81	$C_9H_{19}Cl_2O_5P$	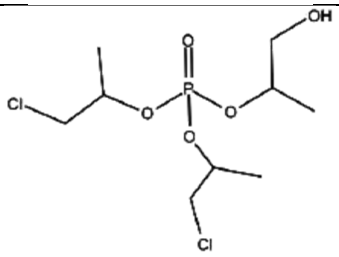	309.0402	309.0348
TCIPP-M2	3.55	$C_6H_{12}Cl_2O_6P$	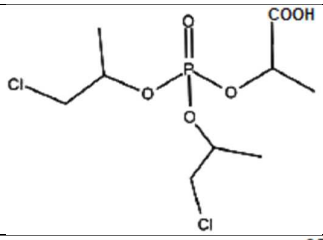	322.9892	323.0140
TCIPP-Glutathione	3.14	$C_{19}H_{34}Cl_2N_3O_{10}PS$	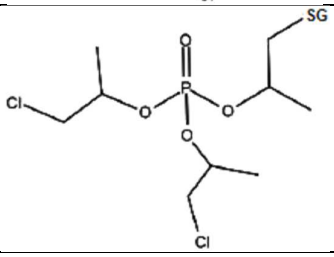	598.1295	598.1080

Table 4: Metabolic profile of TDCIPP by human HepG2 cell lines.

Name	Retention time (mins)	Molecular formula	Chemical structure	Molecular ion $[M+H]^+$	Theoretical mass
TDCIPP	6.52	$C_9 H_{15} Cl_6 O_4 P$	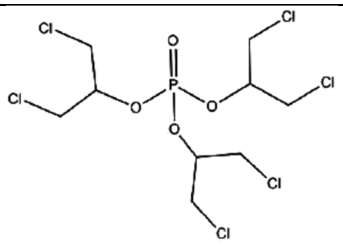	430.8882	430.8809
BDCIPP	2.87	$C_6 H_{11} Cl_4 O_4 P$	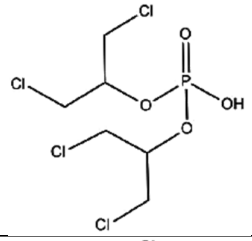	320.9192	320.9120
DCIPP	0.64	$C_3 H_7 Cl_2 O_4 P$	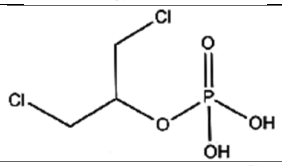	208.9533	208.9459
TDCIPP-M1	4.22	$C_9 H_{16} Cl_5 O_5 P$	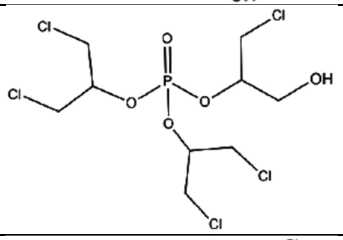	412.9062	412.9149
TDCIPP-M2	3.87	$C_9 H_{14} Cl_5 O_6 P$	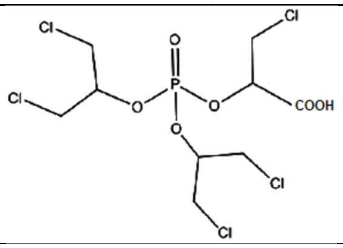	426.8787	426.8942
TDCIPP-Glutathione	3.61	$C_{19} H_{31} Cl_5 N_3 O_{10} P S$	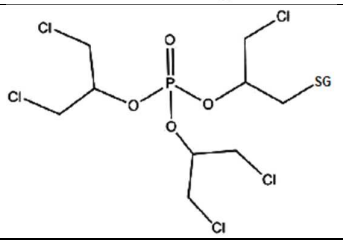	702.0208	701.9982

8 Figures

Figure 1: Chromatographic separation of HBCDs, TCEP, TCIPP and TDCIPP using alternating positive and negative ESI mode.

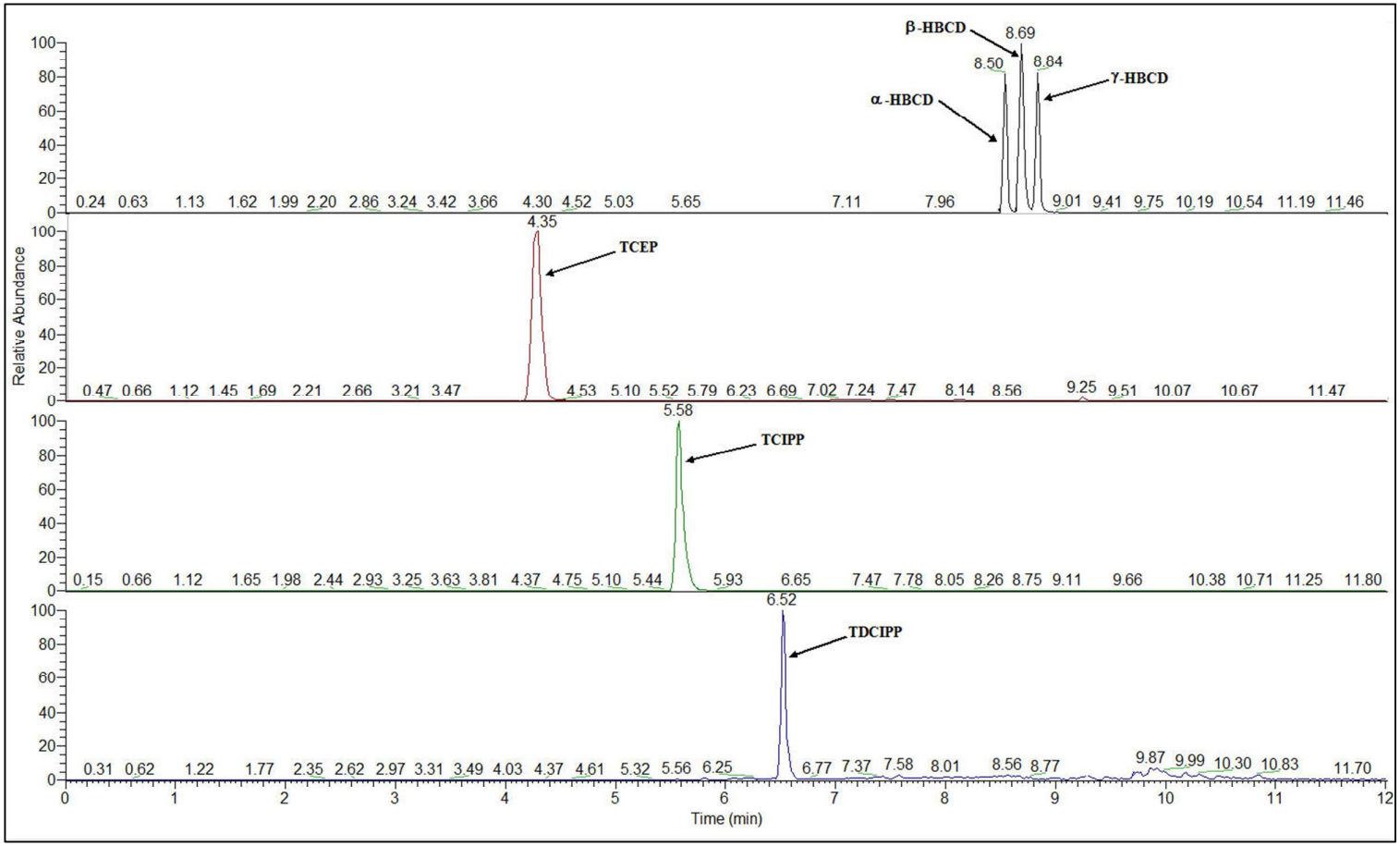

Figure 2: Full scan mass spectra of HBCD, PBCD, TBCD and their mono-hydroxylated metabolites.

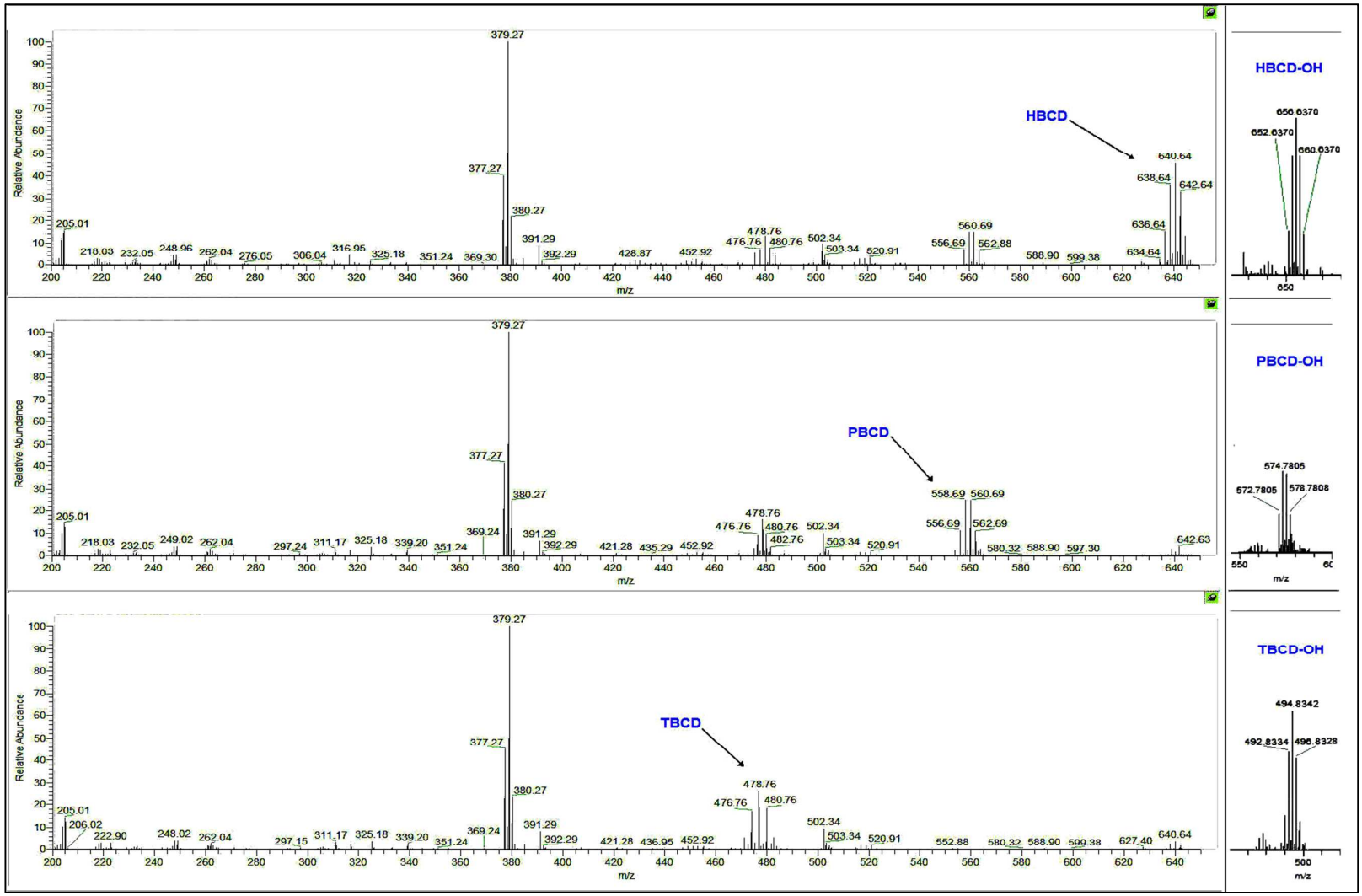

Figure 3: Full scan mass spectra of HBCD and PBCD glucoronide conjugates.

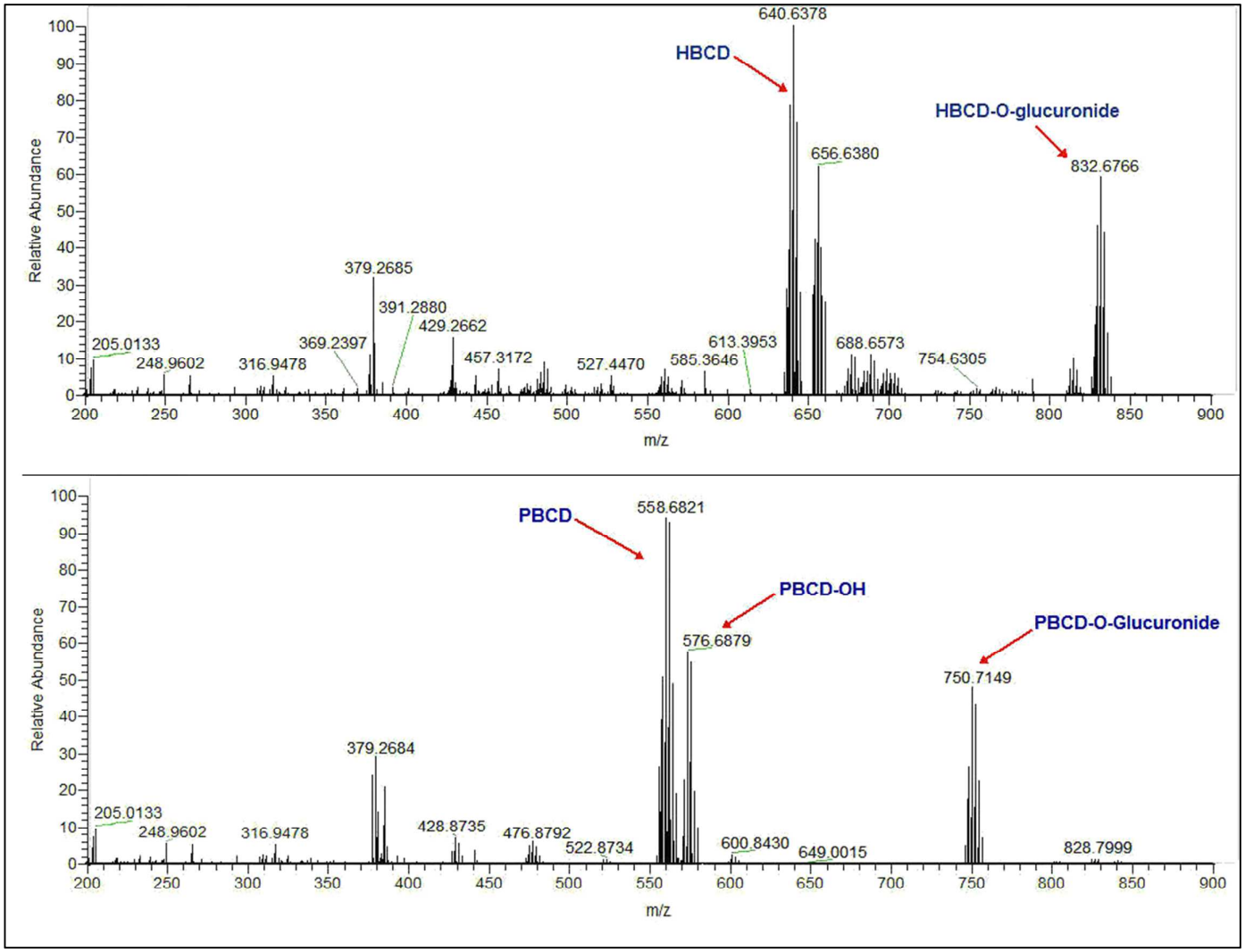

Figure 4: UPLC-Orbitrap™-MS selected ion chromatograms showing TCEP and its metabolites following incubation of indoor dust extract with human hepatocytes for 24 hours.

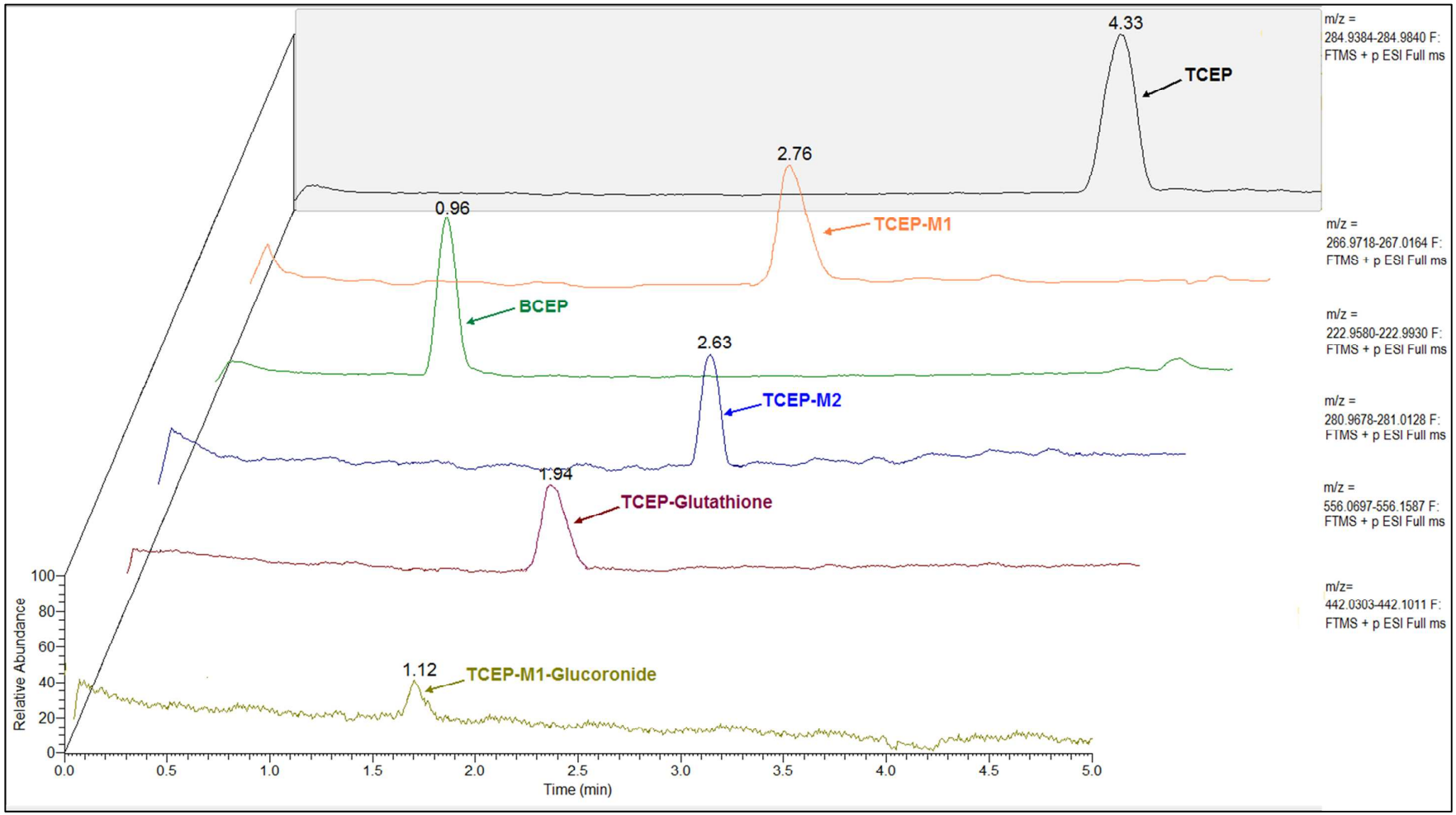

Figure 5: Schematic representation of α-oxidation proposed as a mechanism for biotransformation of TCEP by human hepatocytes.

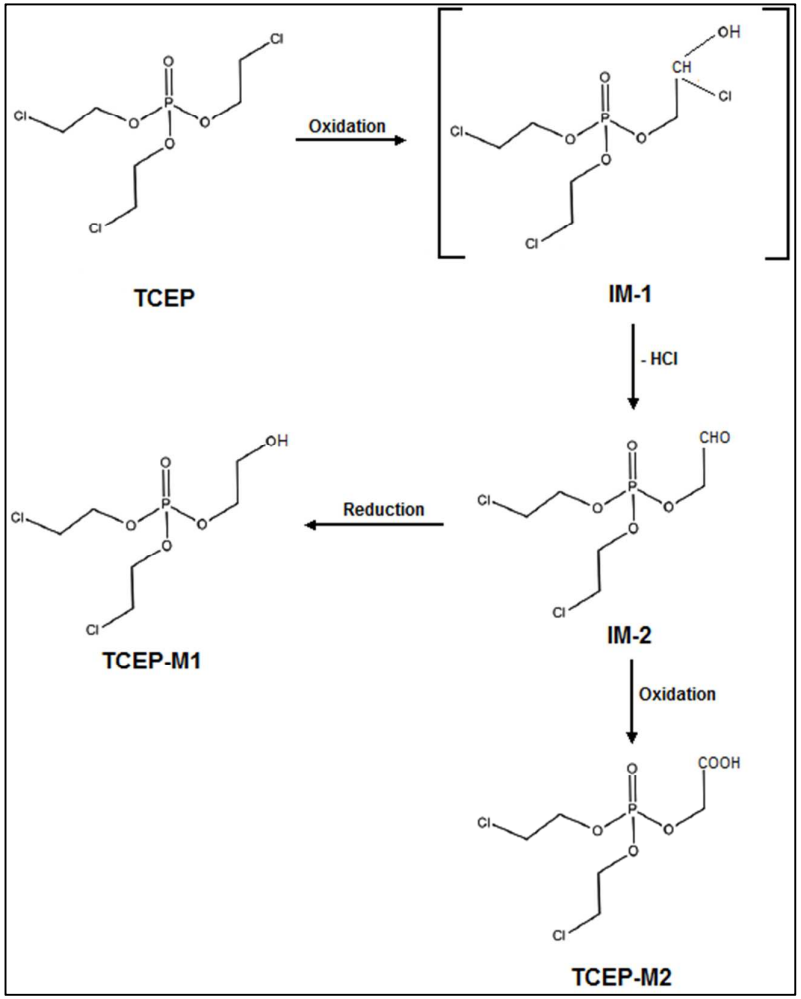

For TOC only.

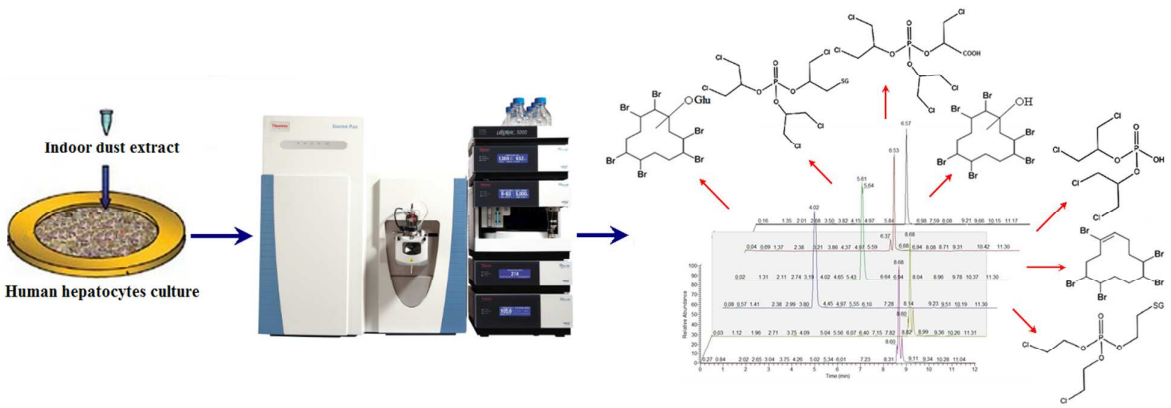

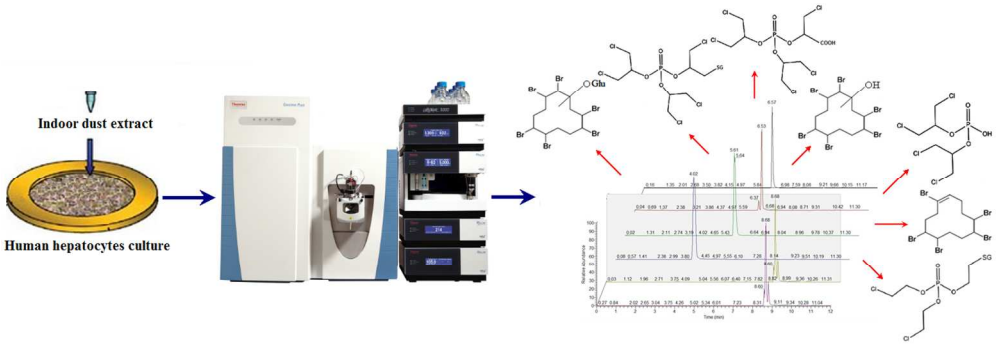

389x135mm (96 x 96 DPI)